Kinetics of Oxygen Binding to Hemoglobin A†

Quentin H. Gibson*

Department of Biochemistry and Cell Biology, Rice University, Houston, Texas 77005

Received December 17, 1998; Revised Manuscript Received February 17, 1999

ABSTRACT: The two-state model [Monod, J., Wyman, J., and Changeux, J. P. (1965) *J. Mol. Biol. 12*, 88−118] postulates a single conformational change which, in the case of hemoglobin, has been related to the structural differences between deoxy and ligated hemoglobins [Perutz, M. F. (1979) *Nature (London) 228*, 726−739]. In its simplest form, the model does not represent satisfactorily either the equilibrium or the kinetics of the hemoglobin−oxygen reaction. The kinetic difficulty is with the rate of dissociation from the T-state, and may be met by assuming a wide difference in behavior between α- and β-subunits. Experiments with Ni−Fe hybrids, however, show almost identical rates of combination with, and dissociation from, the two types of subunit, both of which develop R-like reactions as the pH is raised, the α-Fe-subunits at lower pH than the β-Fe-subunits [Shibayama, N., Yonetani, T., Regan, R. M., and Gibson, Q. H. (1995) *Biochemistry 34*, 14658−14667]. The reactions of oxygen with hemoglobin A and the effect of pH upon them may be represented by assuming behavior of its subunits similar to that of the Ni−Fe hybrids. In such a scheme, α−α and β−β interactions become important elements in cooperativity, and more than two allosteric states are required, for reconsideration of the structural basis of cooperativity.

The two-state model of Monod, Wyman, and Changeux (*1*) has been widely accepted since the classical 1970 paper of Perutz (*2*), offering a convenient and flexible frame for visualizing the reactions of hemoglobin with ligands, and a means of relating structural and functional data. In its simplest form, functional identity of α- and β-subunits is assumed, and the final equation uses five intermediates and three parameters. Opinion has been divided, however, on whether the experimental equilibrium curves were credibly represented by it. The last 10 years have seen significant progress in the application of an expanded model to the equilibrium curve by Ackers and his associates in work recently reviewed in detail (*3*). Estimates of oxygen binding affinity were obtained for all 10 intermediates in a general scheme permitting α−β differences, by measuring dimerization of a range of stable intermediate analogues in which known subunits were blocked by metal substitution or fixed ligands. A wide range of analogues has been examined, and the close correlation of the results appears to validate the conclusions drawn from them (see, e.g., Table 1 of the review cited).

In contrast to the extensive literature on the hemoglobin−oxygen equilibrium, the two-state model has been little applied to kinetics. As the model describes equilibria, it requires supplementary assumptions about the rates of interconversion between the allosteric R- and T-states to extend it to kinetics. These rates have most often been assumed to be fast enough to maintain R- and T-state populations close to equilibrium at all times. This form of the model, applied to a range of data by Hopfield et al. (*4*), though qualitatively adequate, failed to give an acceptable account of oxygen binding kinetics under conditions where the properties of the T-state make a significant contribution to the observed reaction [see Sawicki and Gibson (*5*), Figure 7]. Expansion of the model to include subunit differences increases the number of parameters to be assigned, and this is especially so if rates of R- and T-state interconversion are included. The problem is complicated by the high rates of oxygen dissociation from the T-state which are too great to be followed effectively by the stopped-flow method. Indeed, the existence of a high rate of oxygen dissociation from the T-state was first inferred more by considering the part of the reaction which could not be seen by stopped flow than by observing it [Gibson (*6*)]. The range of times open to study was expanded from the milliseconds of stopped-flow experiments to microseconds by Sawicki and Gibson (*5*). They used laser photolysis of oxygen in hemoglobin solutions at low ligand saturations to observe presumably T-state reactions during oxygen recombination. The results could not be represented by the two-state model, unless a large difference between subunits was assumed, a finding of particular interest in view of the classic paper of Perutz (*2*), who had predicted that ligand binding to β-subunits would be hindered in the T-state.

Using metal−Fe hybrids analogous to those studied by Blough et al. (*7*), oxygen binding kinetics of Ni−Fe hybrids have recently been examined in detail by Shibayama et al. (*8*), and those of Mg, Mn(II), and Cr hybrids (Unzai et al., 1998; *13*). All the work agrees in showing little or no difference between the kinetic parameters of the α- and β-subunits in the T-state, with modest differences in the R-state. The observed reactions of α- and β-subunits may indeed differ widely, depending on pH and effectors, but the difference may depend on changes in the value of the allosteric parameter *L* that defines the ratio of the R- and

† Supported by United States Public Health Service Grant GM 14276.

* Correspondence should be addressed to this author at the Department of Biochemistry and Cell Biology, Rice University, 6100 Main St., Houston, TX 77005. Telephone: 713-737-5777. Fax: 713-285-5154.

10.1021/bi982970t CCC: $18.00
Published on Web 04/02/1999

T-state populations rather than on intrinsic differences in subunit kinetic parameters.

The apparent contradiction between the behavior of metal hybrids and the earlier work with HbA calls for reinvestigation of HbA, not only because of its theoretical interest but also because kinetic information about the subunits is a fundamental requirement for understanding and predicting the properties of genetically engineered hemoglobins. Hybrids with Ni−Fe substitution were chosen because crystal structures, with and without CO as ligand (Luisi and Shibayama, 1989; *9*) are available and because detailed equilibrium studies of normal and $\beta-\beta$-cross-linked hybrids have been reported recently by Shibayama et al. (*19*). This paper shows that the kinetics of native HbA, especially in the T-state, can be represented in a suitable model without invoking subunit differences, by assuming subunit kinetics similar to those of metal hybrids.

EXPERIMENTAL SECTION

Hemoglobin A was obtained by nail bed puncture. A drop of blood was mixed with 5 volumes of distilled water and allowed to stand for 5 min. An equal volume of buffer was then added and the mixture centrifuged in a microcentrifuge for 3 min at maximum (14 000) rpm to remove cell debris and unhemolyzed red cells. The supernatant was further diluted with buffer to the working heme concentration, usually between 0.03 and 0.15 mM.

Photometric observations were made in a 100 mL tonometer fitted with a 1 mm path cell. The sample was first rotated for 5 min with air in the vessel to displace any CO. The tonometer was then flushed with high-purity N_2 introduced through a serum stopper fitted over the tonometer stopcock, and the sample was again rotated. This was repeated, and the tonometer was transferred to the photolysis apparatus to test for the absence of photodissociable species. The peak-to-peak absorbance excursion was always less than 0.001 in absorbance: it was due to photon noise and did not show a systematic trend in the period of observation. The concentration of the sample was measured at this time, often both in a spectrophotometer and in the kinetic apparatus, to establish a relation between the two. The extinction coefficient for deoxyhemoglobin at 430 nm was taken as 145 mM^{-1} cm^{-1}. The values at 436 nm obtained from the kinetic apparatus, with its filters and monochromator, were 115 mM^{-1} cm^{-1} for deoxyHb with a deoxy−oxy difference extinction coefficient of 74 mM^{-1} cm^{-1}. Known concentrations of oxygen were obtained by injecting air from a gastight syringe through the septum and stopcock of the tonometer and rotating for 5 min. The saturation was estimated by measuring the difference spectrum between deoxyhemoglobin and the equilibrated sample, at low fractional saturation, and from readings made in the kinetic apparatus at higher values. The amount of air injected was always less than 10 mL.

Kinetic measurements were made using the apparatus described in some detail by Shibayama et al. (*8*). In outline, the 9 ns photolysis flash was obtained from a Q switched YAG laser (Continuum Inc., Santa Clara, CA). The beam was telescoped to 3 mm diameter and was collinear with the observing beam from a 75 W Xe arc. This passed through a blue glass filter and a 436 nm interference filter, through the sample, into a Spex 250 mm monochromator. The output was recorded with a photomultiplier and amplifier driving a 12-bit 1 μs DAS50 A/D converter (Metrabyte Inc., Taunton, MA) in an IBM PC.

Data reduction and analysis were performed using two models. The first was a conventional Monod, Wyman, and Changeux (*1*) allosteric model as used by Sawicki and Gibson (*5*), with some modifications. In the earlier work, it was assumed that the long dye laser flash had removed all bound oxygen, and as a result the only R-state species present was R-deoxy, which converted to T-deoxy in a short time as compared with any ligand rebinding. With the 9 ns flash, geminate rebinding is extensive, and only a fraction of bound oxygen is released to solvent. To take account of this, photolysis was represented by two parameters describing partial photolysis of R and T species, which are known to have significantly different apparent quantum yields (Morris and Gibson, 1984; *10*). As this model was not used except for control purposes, it is not described further.

The second model was intended to allow the kinetic parameters for the Ni−Fe hybrids to be used in representing the reaction of ligands with hemoglobin A. The two hybrids (α- and β-Fe) require significantly different values of the allosteric constant L when their ligand binding reactions are treated using a two-state model. With HbA it is, therefore, necessary to use two separate two-state ladders, one for each type of subunit. This would yield a maximum value of Hill's n of 2, so in addition to the $\alpha-\alpha$ and $\beta-\beta$ interactions, the doubly liganded α-subunit (R) is allowed to interact reversibly with the singly liganded β-subunit (T) to give a three-liganded R-state intermediate. Other $\alpha-\beta$ interactions could, of course, be specified, but given the difference in the values of L reported by Shibayama et al. (*8*), they would have less effect in increasing cooperativity. The simple scheme described above and shown in Figure 1 has sufficient flexibility in practice to represent the results of experiments with hemoglobin A with good precision. It was assumed that the doubly liganded forms of both subunits were subject to dimerization.

To use the model, the corresponding set of differential equations was solved numerically using values of rate constants for binding and dissociation of oxygen reported by Shibayama et al. (*8*) for Ni−Fe hybrids throughout. Values of other parameters were optimized using a nonlinear least-squares program that was run repeatedly starting with randomly chosen values of each parameter varied. The reactions do not show sufficient response to allow unique values to be assigned to all of the rates of interchange between R- and T-states, but plausible sets of parameters were obtained in every case.

Photolysis of R- and T-States. Morris and Gibson (*10*), using dye laser pulses, showed that different proportions of oxygen were dissociated from these states in hemoglobin A, requiring that two values be assigned in the present experiments. A value for the R-state was obtained by using air-equilibrated hemoglobin A, which, under most conditions, is saturated, and almost wholly in the liganded R-state. The amount of deoxyhemoglobin at the beginning of microsecond observation gives the required quantity immediately. This is not, of course, a quantum yield, but the fraction of the sample dissociated under the conditions of the experiment. This procedure is less satisfactory in providing values for the T-state because it is difficult to find conditions in which

it can be asserted with confidence that oxygen is bound only to the T-state. Addition of inositol hexaphosphate reduces the proportion of R-state species, but may alter the effective quantum yield. Experiments have been performed in which the fraction of oxygen photolyzed was related to initial saturation as measured by static spectrophotometry. The fraction increased at low saturation, with values close to 2 times those found in experiments with the R-state, but the precision decreases seriously under these conditions. Numerical experiment with the model shows that the photosensitivity assumed for the T-state correlates with the value of allosteric *L* which increases as the relative photosensitivity of the T-state is decreased. In some simulations, fractional photolysis of the T-state was included among the variables treated by optimization. The larger amplitude of geminate recombination to α-subunits was also taken into account. Under the conditions of the experiments, the maximum photolysis of oxygen observed was 30%.

Although the scheme requires 18 parameters, for the present purpose many of these can be assigned beforehand, or have minor effects on the course of the computed reaction. To begin with, the four rates for oxygen binding to, and release from, the T-state have been taken from Shibayama et al. (*8*), the R-state off rates from Olson et al. (*20*), the R-state on rates from Unzai et al. (*13*), and analysis of small-amplitude flash photolysis experiments at high oxygen concentrations. The tetramer−dimer dissociation constant has been assigned a value of 1 μM (see ref *3*), and the fraction of R-state species dissociated by the flash was determined in separate experiments. The rate at which the conformation of the triply liganded species can return from R to T has relatively little effect on the kinetics, though the ratio of forward and reverse rates influences equilibria, and must also be included to maintain reversibility. The rate of appearance of the triply liganded R-state species is significant, however, and has been assigned by optimization. It has the dimensions of a second-order reaction as the diliganded α-dimer reacts with the monoliganded β-dimer (Figure 1). The scheme includes explicit rates of interchange between R- and T-states. Relatively little is known about these rates, though they are known to be strongly dependent on pH, increasing markedly under acid conditions [Sawicki and Gibson (*5*)]. It has been assumed that as ligand binding proceeds the R to T and T to R rates decrease and increase, respectively, by the same factor at each step, i.e., equal energy changes. The program was run from 50 to 500 times with randomly chosen starting values of the parameters being optimized. It is difficult to give estimates of the precision of the individual parameters, since the errors calculated from the residuals are influenced by the assumption that the ligand binding and dissociation rates are precisely known. The fits obtained show that the scheme is capable of representing the reactions well, but the values may not be unique.

RESULTS AND DISCUSSION

Reaction Scheme. To relate values for the ligand binding reactions of the Ni−Fe hybrids to the behavior of native hemoglobin, the scheme of Figure 1 was adopted. The α- and β-subunits are allowed to make functional allosteric transitions independently of one another. As in the metal hybrids, the interactions are α−α and $\beta-\beta$ with the additional assumption that the doubly liganded α-species

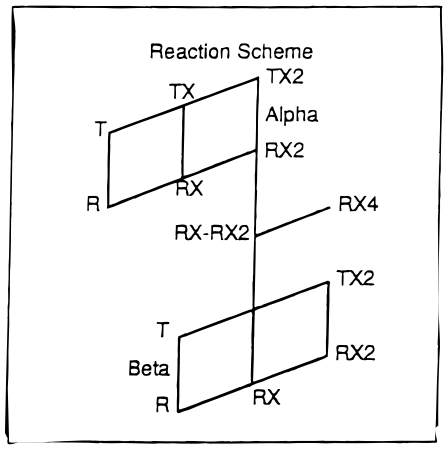

FIGURE 1: Scheme used for computation. R (R-state) and T (T-state) identify the type of ligand binding behavior associated with each species. T-state parameters were fixed at 6.5 μM^{-1} s^{-1} and 2000 s^{-1} for combination and dissociation throughout: the values were taken from Shibayama et al. (*8*), and used for both α- and β-subunits. The R-state combination rates were set at 36 μM^{-1} s^{-1} for α-subunits and at 72 μM^{-1} s^{-1} for β-subunits. These rates reflect literature values for the subunits and for HbA tetramers [see Unzai et al. (*13*) for references]. The rates of oxygen dissociation were 12 and 21 s^{-1} for α- and β-subunits, respectively, from Olson et al. (*20*). X is a ligand molecule. Each vertical line between R and T denotes an interconversion between allosteric states defined by R to T and T to R rates. The rates in each direction increase (T to R) and decrease (R to T) by $c^{1/2}$ as each ligand is added, where $c = R_{on}T_{off}/T_{on}R_{off}$. Species α-RX2 and β-TX interact to give R-state Hb4X3. A list of rates is given in the Appendix.

interacts, reversibly, with the singly liganded β-species to form an R-state triply liganded species. The choices made reflect earlier observations on CO binding of hemoglobin by Marden et al. (*11*), who followed CO rebinding spectrophotometrically following flash photolysis, as well as binding and release of the fluorescent effector pyrene trisulfonate, which binds some 60 times more strongly to deoxy than to liganded hemoglobin. They found that R-state rates of ligand binding appeared earlier in the reaction than the two-state model will permit and also observed release of pyrene trisulfonate at rates corresponding to R-state rates of CO binding. They concluded that there must be an additional state or states in which pyrene trisulfonate is bound (a T-state characteristic) but which also reacts rapidly with CO as though in the R-state. The anomalous state was identified with the doubly liganded tetramer.

Oxygen Recombination in pH 7.1 Phosphate Buffer at Low Initial Saturation. Two sets of data that agree well with the earlier data of Sawicki and Gibson (*5*) are illustrated in Figure 2. Panel A shows the effect of varying hemoglobin concentration at constant pO_2, and panel B gives the results of varying oxygen concentration with constant hemoglobin. The continuous lines have been generated from the scheme described in the Experimental Section, with the assumption that the T-state rates of bimolecular combination and dissociation of oxygen are identical for the two types of subunit and have the numerical values suggested by Shibayama et al. (*8*) for the Ni−Fe hybrids. The fits are good, and the equilibrium curve and cooperativity of hemoglobin A are well-represented with a *n* value of 2.76. However, as reported earlier (*5*), good fits with root-mean-square residuals as low as 0.00025 in absorbance can be obtained for the same data with the two-state model, if the subunits are

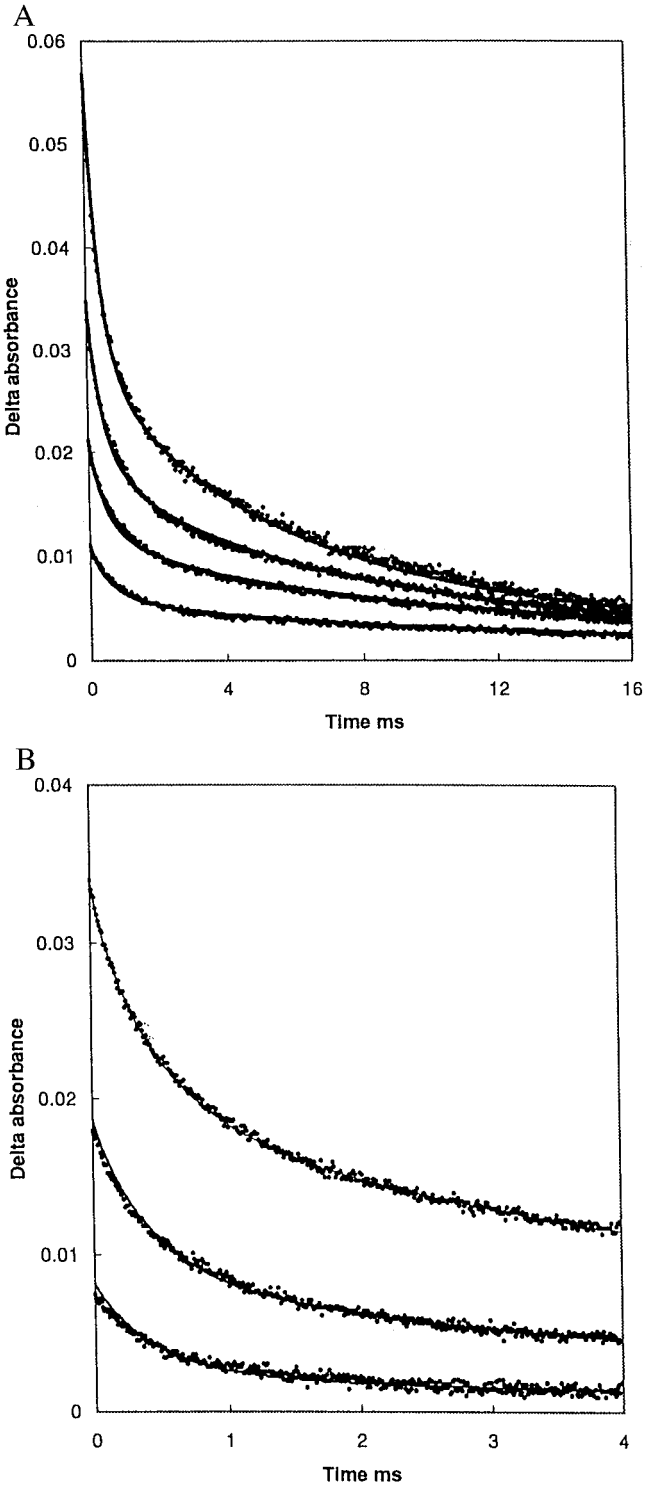

FIGURE 2: (Panel A) Absorbance changes following photolysis of oxyhemoglobin in equilibrium with 13.1 μM O_2, Hb (5.2, 9.2, 17.1, and 25.8 μM tetramer), and 0.1 M KPi, pH 7.0, with 0.3 mM EDTA, 21 °C, 436 nm. Parameters: $L_{0\alpha} = 6680 \pm 83$, $L_{0\beta} = 10\,300 \pm 210$, RX2(α−α)+TX($\beta$) (rate 12°), 625 ± 51, $R_{0\alpha} \rightarrow T_{0\alpha} = 26\,400 \pm 1600$, $R_{0\beta} \rightarrow T_{0\beta} = 243\,000 \pm 17\,000$. Other parameters as in the Appendix list. (Panel B) Hb (14.0 μM) and O_2 (5.2, 10.4, 15.6 μM). Parameters: $L_{0\alpha} = 18\,300 \pm 116$, $L_{0\beta} = 25\,800 \pm 214$, RX2(α−α)+TX(($\beta$) (rate 12°), $3\,855 \pm 42$, $R_{0\alpha} \rightarrow T_{0\alpha} = 445\,000 \pm 29\,000$, $R_{0\beta} \rightarrow T_{0\beta} = 295\,000 \pm 2500$. Other parameters as in the Appendix list.

allowed to have different rates of O_2 binding and dissociation. The two phases of the recombination reaction that led Sawicki and Gibson (*5*) to assign different T-state reaction

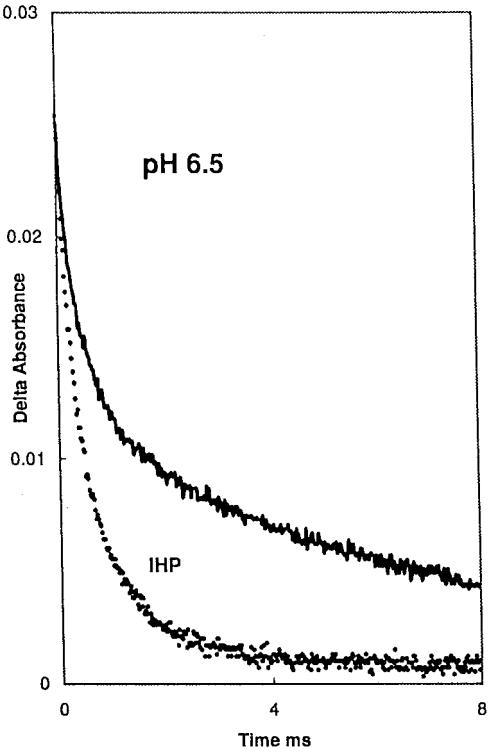

FIGURE 3: The upper line shows the time course of oxygen recombination following photolysis of 23.7 μM hemoglobin in 0.1 M KPi + 0.3 mM EDTA, pH 6.5, equilibrated with 13.1 μM O_2. Other conditions as for Figure 4. The lower time course is for the same solution after the addition of 0.1 mM inositol hexaphosphate. Parameters: $L_{0\alpha} = 12\,700 \pm 351$, $L_{0\beta} = 4\,570\,000 \pm 10\,000\,000$, i.e., large but undefined, RX2(α−α)+TX(β) (rate 12.) 2340 ± 103, $R_{0\alpha} \rightarrow T_{0\alpha} = 26\,4005 \pm 1600$, $R_{0\beta} \rightarrow T_{0\beta} = 259 \pm 564$.

rates to the subunits are obvious in Figure 2. Their proposal, however, conflicts with the kinetic results for Ni−Fe, Mn(II)−Fe, and Mg−Fe hybrids which have led to closely similar rates for the R- and T-states of the α- and β-subunits (*8*, *13*). The oxygen equilibrium and subunit assembly experiments recently reviewed by Ackers (*3*) for a large number of hybrids also indicate cooperative interactions in the binding of the first two ligand molecules, without subunit differences. The schemes differ in that the interactions observed in kinetic experiments with the hybrids studied are between like (α−α and β−β) pairs of subunits rather than the α−β interactions of Ackers' scheme. In kinetic experiments with hemoglobin A, this is a distinction without a difference as the subunits can scarcely be resolved by optical spectroscopy.

Effect of pH on Recombination. The scheme predicts that at extremes of pH the marked biphasicity of the data of Figure 2 should decrease, and this is observed experimentally (Figure 3). The model gives a good fit to data at pH 6.5 (a modest change in pH in this context) with modified allosteric parameters. Two groups of solutions were obtained: in one, the interaction between unlike subunits is decreased, and the R to T rates associated with the two L_0 values are different, with lower rates for the α-subunit. The L_0 values for like pairs are little changed. In the other group of solutions, the L_0 value for the β-subunit is large enough for it to remain in the T-state throughout, and the interaction between unlike subunits becomes more important. The addition of inositol hexaphosphate at pH 6.5 has an effect much larger than that of the pH change alone, with almost complete disappearance

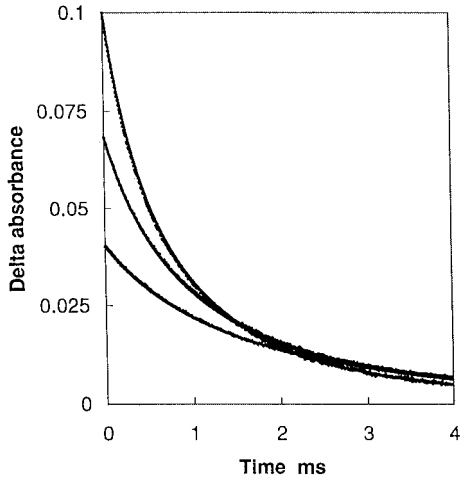

FIGURE 4: Oxygen binding to 18.6 μM HbA in 0.1 M borate buffer, pH 9.1, with 2.6 μM O_2. Parameters: $L_{0\alpha} = 66$, $L_{0\beta} = 44$. Relative photolysis intensities of 1, 0.25, and 0.0625. Data points at intervals of 10 μs. Rates of ligand reactions are as in the list in the Appendix; other conformational parameters are ill-defined (see text).

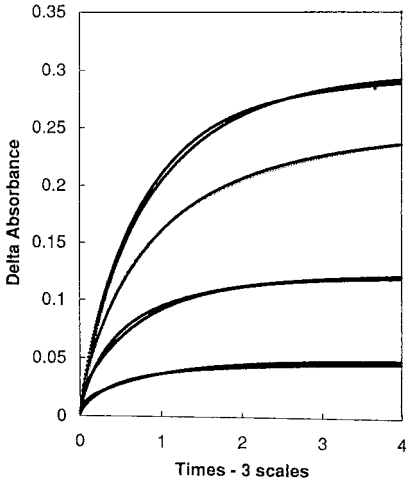

FIGURE 5: Representation of stopped-flow data of Gibson (*6*) by Figure 1. The data were recovered using the descriptive rate constants assigned at that time. Data and computed values are joined by lines. The rms residual was 0.0021 in absorbance, or 0.68% of the excursion measured. From top to bottom, the initial $[O_2]$ values were 124, 62, 31, and 16.5 μM. The reactions were followed for 10, 20, 40, and 40 ms, respectively. The original experiments were performed using 0.1 M KPi buffer, pH 7.0 at 20 °C. Parameters: $L_{0\alpha} = 1700$, $L_{0\beta} = 4600$, RX2($\alpha-\alpha$)+TX(β) (rate 12.) 17.4, $R_{0\alpha} \rightarrow T_{0\alpha} = 140\,000$, $R_{0\beta} \rightarrow T_{0\beta} = 95\,000$. Other values are from the Appendix list; so many other sets of values are possible. The experiment shows that the equilibrium curve can be well reproduced (rms residual 0.48%) with ligand affinities taken from Ni−Fe hybrids.

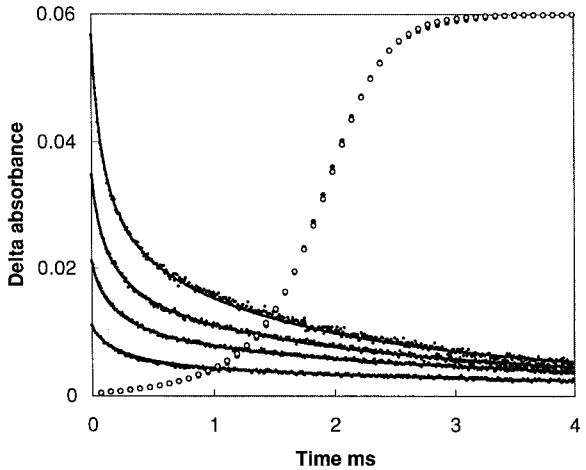

FIGURE 6: Simultaneous fit of kinetic and equilibrium data. The equilibrium curve has been scaled to fit the frame of the figure; the filled circles are experimental, the open circles computed. The parameter values used are given in the Appendix, and the kinetic data were taken from Figure 4 with additional data (not shown) from Figure 8. The highest correlation was between L_α and L_β (0.73); all other correlations were significantly smaller. Note that all standard errors are much smaller than in other computer runs.

of the slower phase of the reaction (Figure 3). This result may be represented by increasing the values of allosteric L_α and L_β while retaining equivalence of subunit T-state kinetic parameters with the same numerical values as for the experiments at pH 7.1. Under these conditions, the R-state parameters are poorly defined as the state is scarcely populated. Taking the experiments with and without inositol hexaphosphate together, it seems that the experiments at pH 6.5 without effector are better represented by the second parameter set.

The scheme shown in Figure 1 is also successful in describing experiments using borate buffer at pH 9.1. The values of both L_α and L_β must be reduced by a factor of about 100 to give the fits of Figure 4, though their relative sizes are not well determined. As the affinity is so high at pH 9, very small amounts of oxygen were needed, and the data are for relatively high initial saturations. It is possible to fit data from a wide range of initial saturations in experiments at high pH because the behavior of the T-state is only marginally relevant. It was this circumstance which allowed Hopfield et al. (*4*), using a basic two-state model, to represent stopped-flow data of Gibson (*6*) for oxygen combination at high pH with fair success, while failing seriously with experiments at pH 7.

In view of this problem, it is of interest to see if the scheme of Figure 1 is consistent with the pH 7 stopped-flow data. It was found that the data may be reproduced with relatively small errors (Figure 5). As the raw 1970 data are no longer available, traces were generated from the best-fitting parameter values of the kinetic equivalent of the Adair (*14*) equation used at the time. The treatment then used included extrapolation to the absorbance value at the time of mixing. This is an important quantity in stopped-flow work with the oxygen reaction as, at the highest $[O_2]$ used, nearly 50% of the observed reaction took place during the dead time of the apparatus so the results shown in Figure 5 are much better than might have been expected. The reactions were followed nearly to equilibrium, so it is evident that Figure 1 is able to reproduce the equilibrium curve as well as the kinetics. This has been confirmed by fitting an equilibrium curve for HbA obtained under the conditions of the 1970 experiments (R. J. Morris and Q. H. Gibson, unpublished). The two L parameters and the $\alpha-\beta$ interaction parameters were varied. A good fit was obtained over a wide range of oxygen concentrations, but the correlation between the parameters is so high that other sets of parameters are acceptable if the equilibrium curve is treated alone.

This situation was greatly improved by fitting kinetics and equilibria together. As may be seen by comparing Figure 2 and Figure 6, the fit to the kinetic data is scarcely impaired, but the indicated errors in parameters (see Appendix) are greatly reduced and only 1 solution was found in more than

200 trials with different initial parameter values. The subunit L values, the $\alpha-\beta$ interaction parameter, and the rates of R−T interconversion were varied.

Flash Photolysis of Fully Liganded Hemoglobin. Although the rate of binding of oxygen to $Hb_4(O_2)_3$ has been measured by numerous authors (see ref *22* for references), new experiments with the present buffer and apparatus were performed to give an estimate of the rates to be used in curve-fitting. As the concentration of oxygen is usually substantially greater than that of hemoglobin, the rate of the recombination reaction may be expected to be proportional to oxygen concentration. This, however, turned out to be only partly true even when the reaction was followed after photolysis of as little of 2% of the combined oxygen. Data were collected over a 128-fold range of light intensities and a 4-fold range of oxygen concentrations. The resulting families of eight records at each oxygen concentration could be fitted by the scheme of Figure 1 with a root-mean-square residual of less than 0.0005 in absorbance (Figure 7A,B). The time course of recombination is biphasic, as expected, both because partial flash photolysis will always yield a mixture of intermediates, and because the main photoproduct at low fractional photolysis, $Hb_4(O_2)_3$, may switch from the R- to the T-state fast enough to compete with recombination with oxygen. The amplitude of the slower phase, however, is larger than had been anticipated, probably because of the use of a phosphate buffer. To compare the observed and computed time courses, each was fitted to a sum of two exponentials, giving rates and amplitudes for both components. When the data are treated in this way, the faster component corresponds to a second-order rate of 55 μM^{-1} s^{-1}, in good agreement with earlier work. The slower component yields an apparent second-order rate declining from 10 to 3.5 μM^{-1} s^{-1} as the oxygen concentration decreased from 262 to 62 μM. Figure 8 compares observed and computed rates and amplitudes for these preflash oxygen levels. The scale for the slower component with 5% O_2 has been increased 5-fold to show the results more clearly. Both faster and slower second-order rates are largely independent of fractional photolysis in the range accessible with a short flash.

The percentage of the slow reaction at each light level is also shown in Figure 8, and is larger with 5% O_2 than with air. The percentage trends downward as the flash intensity is decreased, changing more than 2-fold with 5% O_2 (Figure 8, panel B). These results are consistent with a contribution to the slow rate from an intermediate relaxing from fast to slow (from R to T) in competition with oxygen rebinding. As the slower component retains about half its amplitude even below 2% photodissociation, in the two-state model this intermediate can only be $Hb_4(O_2)_3$. The effect of oxygen concentration on the slower apparent second-order rate is consistent with this. The observed rate depends both on the rate of the transition of $Hb_4(O_2)_3$ from R to T and on the rate of oxygen rebinding. At the higher oxygen concentration, if the transition is limiting, the second-order rate would be expected to be greater at the higher $[O_2]$.

The experiments of Figures 7 and 8 may be represented by Figure 1 with R-state on rates for oxygen binding to α- and β-subunits of 37 and 72 M^{-1} s^{-1}, respectively, close to the values reported by Unzai et al. (*13*) for subunits in Cr hybrids. The two-state model, expanded to admit subunit differences and with finite rates of interconversion between R- and T-states, is also able to reproduce the data of Figures 7 and 8 with much the same goodness of fit as is shown there. The implication is that $Hb_4(O_2)_3$ divides between R- and T-states, equilibrating in a time of the same order as that required for oxygen recombination, as suggested by the experiments of Ferrone and Hopfield (*12*) with HbCO. The two-state model requires, however, that as each ligand

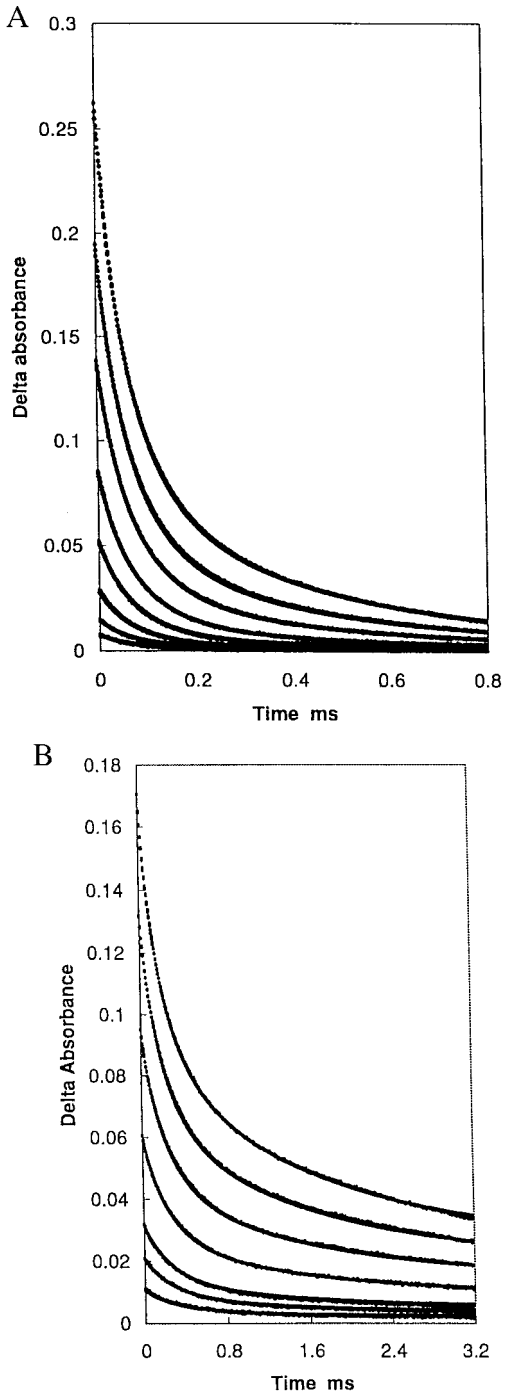

FIGURE 7: Flash photolysis of HbA at high initial saturation with oxygen and various light levels. Panel A, initial $[O_2] = 262$ μM; panel B = 62.5 μM. Interval between data points: (A) 2 μs; (B) 8 μs. (A) HbA = 33.6 μM; (B) HbA = 30.3 μM tetramer. Relative light intensities: 1, 0.5, 0.25, 0.125, 0.0625, 0.0313, 0.0156, and 0.0078. Buffer: 0.1 M KPi, pH 7.0, with 0.3 mM EDTA. Parameters: $L_{0\alpha} = 219 \pm 126$, $L_{0\beta} = 4160 \pm 429$, RX2(α−α)+TX-($\beta$) (rate 12°) = 654 ± 34, $R_{0\alpha} \rightarrow T_{0\alpha} = 26\,400 \pm 1600$, $R_{0\beta} \rightarrow T_{0\beta} = 1\,160\,000 \pm 100\,000$. Other values from the Appendix list.

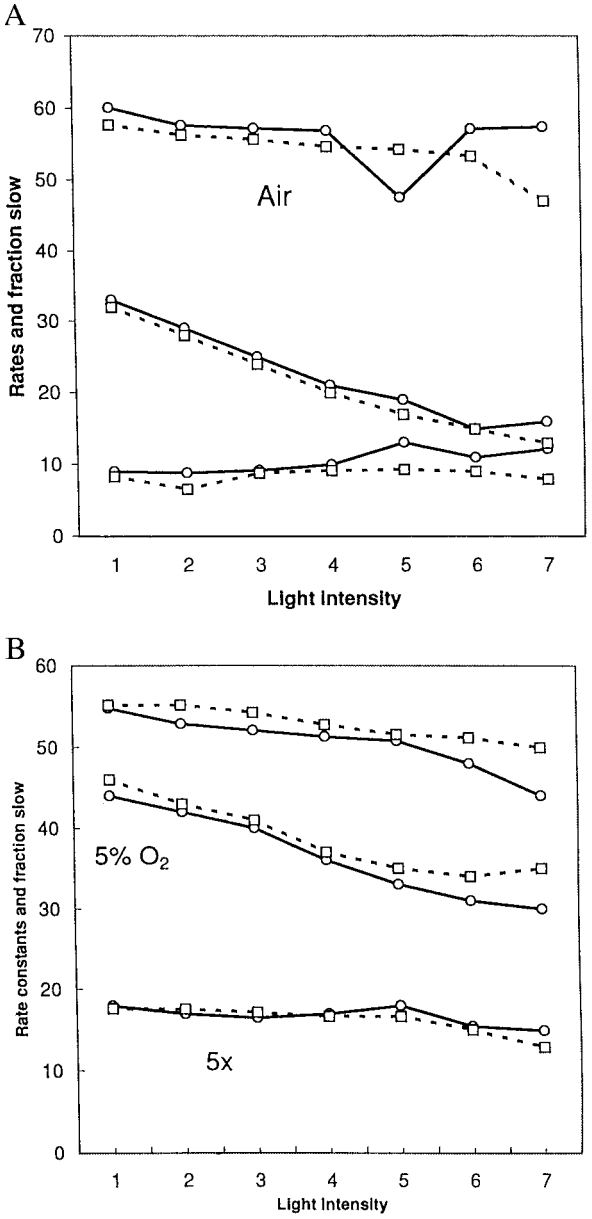

FIGURE 8: Analysis of data from Figure 2. In both panels, the continuous lines refer to experimental data, the dashed lines to computer representations. From top to bottom in both panels, the top pair represent the second-order rate of the faster component in units of μM^{-1} s^{-1}, the lowest pair the second-order rate of the slower component in the same units. Note that the data of this line in panel B have been multiplied by 5 to improve clarity. The middle pair of lines gives the percentage of the total absorbance change contributed by the lower rate. Abscissa: the light was halved at each step from 2 to 7.

molecule is removed the T-state be favored relative to the R-state by allosteric *c*, the ratio of the oxygen affinities of R- and T-states. This has a value on the order of 500, so if the three-liganded form has a significant proportion of T-state at equilibrium, the two-liganded form must be almost entirely in the T-state, a conclusion at variance with the experiments of Ackers (*3*), the kinetic experiments of Marden et al. (*11*), and the requirements of the kinetic Figure 1 of this paper.

The Model Scheme in Relation to Other Experiments. Subunit equivalence in the T-state is a basic element in the new scheme, and it is necessary, therefore, to examine the consistency of this assumption with other experimental evidence. Many equilibrium experiments of several types, reviewed by Ho (*15*), have usually suggested equilibrium differences less than 2-fold between α- and *β*- subunits in the T-state. The experiments are inherently difficult because the cooperativity of mammalian hemoglobins is so high that the population of intermediates with a single ligand, critical for assessing the relative affinities of the subunits in the T-state, is always small even at low fractional saturation.

Nevertheless, Figure 1 with the parameter values in the Appendix appears substantially consistent with NMR data (*15*, *23*, *24*). Signals correlated with the α- and *β*-subunits in the unliganded T-state disappeared in parallel on partial oxygenation in phosphate-free buffers. With phosphate or effectors, the α-subunit signal was lost earlier than that from the *β*-subunit. Interpretation of the results called for cooperativity within the T-quaternary structure; i.e., they were not consistent with the two-state model. Very different experiments on crystals of HbA and on HbA in silica gels, however, showed noncooperative binding and a 5-fold difference in subunit affinity (*25*, *26*). No clear choice can be made at present from the range of possible explanations of this interesting result which is not consistent with Figure 1.

The structures of the subunits revealed by crystallography, on the other hand, are significantly different, a difference that led Perutz (*2*) to conclude that ligands could not bind to *β*-subunits in the T-state, and to make this an element in his classical interpretation of the two-state model of Monod et al. (*1*) in structural terms. Direct kinetic evidence for HbA is limited to experiments with CO as ligand that are much easier to perform than experiments with oxygen, but these experiments have consistently failed to show any evidence of significant α−*β* differences. For example, experiments with hybrid hemoglobins in which protoheme of specific subunits was replaced either with meso- or with deuteroheme showed no α−*β* differences [Parkhurst et al. (*16*)], as well as experiments with hybrids in which Fe in specific hemes has been replaced by other metals (*7*, *8*, *13*). Further convincing evidence in favor of α−*β*-equivalence in the T-state has been given in Table 1 of the review of Ackers (*3*).

Mechanism of Figure 1. The main difficulty in representing oxygen kinetics has always been to account for the slower second phase in rebinding of oxygen at low fractional saturation. In Figure 1, it is modeled by rearrangement of ligands among binding sites from their initial kinetic distribution to an equilibrium distribution favored by cooperativity. As compared with the two-state model, Figure 1 favors the distribution reaction because, with suitable values of *L*, R-state behavior appears much earlier in the reaction. The difference in the *L* values for α- and *β*-subunits suggested by the Ni−Fe hybrids is an important element of flexibility in curve-fitting operations. It enhances the slower secondary phase, because the *β*-subunits, which have the larger value of *L* and are more likely to remain in the T-state, can give up ligand to the α-subunits, which by switching to the R-state retain it. This mechanism, of course, is applicable only when hemoglobin is in large excess over ligand, as in the old experiments of Sawicki and Gibson (*5*).

In terms of the model, the effect of pH on the *L* values of the subunits is large, and at low pH and in the presence of inositol hexaphosphate, hemoglobin remains largely in the T-state until much higher saturations have been reached. The

intrinsic similarity of subunits in the T-state is more fully expressed, the observed rate constant for approach to equilibrium with ligand is increased, and the recombination reaction with oxygen approximates closely to a single exponential (Figure 3). These features are reproduced in Figure 1 by increase in the values of *L* for both types of subunit. Conversely, at high pH, binding of a ligand by deoxyhemoglobin is associated with an immediate change of affinity, modeled by drastic reduction in the values of *L* for both subunits.

The model has two three-member two-state arrays. As this would lead to a maximum value of 2 for Hill's *n*, interaction between the arrays as well as within them is needed to reach a higher value. In the interest of simplicity, only a single step has been added, and again based on the Ni−Fe hybrids, it is assumed that a doubly liganded α-subunit, if in the R-state, can interact with a singly liganded β-subunit in the T-state, raising the probability of conversion of the remaining unliganded β-subunit to the R-state. This step should correlate with the major structural changes described by Perutz and his associates (*2*). That change, however, though still associated with cooperativity, would now have a secondary role, with most cooperativity in Figure 1 arising from interactions between like subunits. Calculation shows that much of the total cooperativity of HbA must arise from intradimer reactions with values of *n* within the dimer greater than 1.5. This is not consistent with the low *n* values for the Ni−Fe hybrids reported by Shibayama et al. (*18*), who, in experiments with 4 μM hemoglobin, found *n* greater than 1 only for the α-Fe hybrid, with the slope of the Hill plot increasing above 50% saturation. More recently, experiments with cross-linked hybrids (Shibayama et al., 1995; *19*), where dimerization is not a factor, have yielded values of *n* up to 1.75, consistent with the calculations using Figure 1. It has always seemed unlikely that a single change in structure would account for the complex allosteric behavior of hemoproteins, and evidence of this kind is beginning to appear, Ansari et al. (*17*), for example, seeing multiple absorbance changes even in myoglobin. Relating kinetic models and structure is always speculative, and even excellent ability to reproduce experiments does not prove a model correct. With this proviso in mind, Figure 1 has worked well in a wide range of conditions, but should nevertheless be applied cautiously in experiments at high hemoglobin saturation. It will be clear from the Experimental Section that the rates assigned to the R−T interchanges are not always well-defined and the precise values for them included in the figure legends are given for completeness only. In general, however, large values for R to T rates are usually found in optimization.

Although the model was developed in relation to the specific question of the applicability of data from metal hybrids to T-state hemoglobin A, flash experiments with saturated oxyhemoglobin could also be modeled, and even the calculated rate for the oxyhemoglobin dithionite reaction measured 28 years ago (*6*) was readily simulated.

It is particularly interesting to compare Figure 1 with the models of Ackers and his associates (*3*). As already mentioned, though differing in detail, both suggest strong cooperative interactions within dimers, with significant R-state behavior of the doubly liganded species which is a major point of difference from the predictions of the simple two-state model. Thus, the kinetic experiments described here and the equilibrium and subunit assembly experiments appear to reinforce one another. In the same connection, experiments carried out more than 40 years ago by Gibson and Roughton (*21*) on the kinetics of CO binding to sheep hemoglobin, when analyzed in terms of four consecutive reactions, required a larger than statistical value for the rate of binding the second molecule, as is consistent with Scheme 1.

In sum, the behaviors of hemoglobin A and of the Ni−Fe hybrids are consistent with one another, and an extension of the two-state model, based on the behavior of the Ni−Fe hybrids, can account for the kinetics of the principal reactions of HbA with oxygen.

ACKNOWLEDGMENT

It is a pleasure to thank Dr. J. S. Olson for many interesting discussions and for reading this paper before submission.

APPENDIX

List of Parameter Values from the Data of Figure 7. 1. and 2. $L_{0\alpha}$ and $L_{0\beta}$, 5400 ± 110 and 20 000 ± 470, respectively; 3. and 4. α and β T-state on rates, fixed throughout at 6.5 μM^{-1} s^{-1}; 5. and 6. α and β R-state on rates, 36.0 ± 0.2 and 78 ± 0.64 μM^{-1} s^{-1} for α and β, respectively; 7. and 8. α and β T-state off rates, fixed at 2000 s^{-1}; 9. and 10. α and β R-state off rates, fixed at 12 and 20 s^{-1}, respectively; 11. tetramer−dimer dissociation constant, fixed at 1 μM; 12. rate of $\alpha\beta$ interaction and T to R change of β-TX → β-RX, 3 400 ± 310; 13. reverse of reaction 12., often fixed at 10 000 s^{-1}; 14. and 15. rates $R_0 \rightarrow T_0$ for α and β, 1600 ± 29 and 142 000 ± 5600, respectively; 16. photolysis efficiency for α-subunits, breakdown set at 0.7 of β amplitude to allow for difference in geminate recombination; 17. photolysis efficiency for T-state subunits, 0.5; 18, photolysis efficiency for β-subunits, 0.23.

Correlation of Parameters. The model of Figure 1 has the problem that the cooperativity inherent in the difference between the R- and T-state affinities is expressed in two ways. It may appear in the *L* values and in parameters 12. and 13. which describe the α−β interaction. The result is a high correlation between these parameters and comparable fits to data with divergent parameter values. When this occurs, less extreme values have been selected.

Standard Errors. It is not possible to give sound estimates of standard errors because their calculation assumes that fixed parameter values are precisely known. Further, residuals are assumed to be normally distributed, which is another way of saying that the model correctly describes the data. In most cases, however, standard errors have been included in the figure legends because their relative sizes give some indication of the sensitivity of the fits to specific parameters. Note that the solutions were highly constrained when equilibria and kinetics were fitted together.

REFERENCES

1. Monod, J., Wyman, J., and Changeux, J.-P. (1965) *J. Mol. Biol. 12,* 88−118.
2. Perutz, M. F. (1970) *Nature (London) 228,* 726−739.
3. Ackers, G. K. (1998) *Adv. Protein Chem. 48,* 185−253.
4. Hopfield, J. J., Shulman, R. G., and Ogawa, S. (1971) *J. Mol. Biol. 61,* 425−443.

5. Sawicki, C. A., and Gibson, Q. H. (1977) *J. Biol. Chem. 252*, 7538−7547.
6. Gibson, Q. H. (1970) *J. Biol. Chem. 245*, 3285−3288.
7. Blough, N. V., Zemel, H., and Hoffman, B. M. (1984) *Biochemistry 23*, 2883−2891.
8. Shibayama, N., Yonetani, T., Regan, R. M., and Gibson, Q. H. (1995) *Biochemistry 34*, 14658.
9. Luisi, B., and Shibayama, N. (1989) *J. Mol. Biol. 206*, 723−726.
10. Morris, R. J., and Gibson, Q. H. (1984) *J. Biol. Chem. 259*, 365−371.
11. Marden, M. C., Hazard, E. S., and Gibson, Q. H. (1986) *Biochemistry 25*, 7591−7596.
12. Ferrone, F. A., and Hopfield, J. J. (1976) *Proc. Natl. Acad. Sci. U.S.A. 73*, 4497−4501.
13. Unzai, S., Eich, R., Shibayama, N., Olson, J. S., and Morimoto, H. (1998) *J. Biol. Chem. 273*, 23150−23159.
14. Adair, G. S. (1925) *J. Biol. Chem. 63*, 529−545.
15. Ho, C. (1992) *Adv. Protein Chem. 43*, 152−312.
16. Parkhurst, L. J., Geraci, G., and Gibson, Q. H. (1970) *J. Biol. Chem. 245*, 4131−4135.
17. Ansari, A., Jones, C. M., Henry, E. R., Hofrichter, J., and Eaton, W. A. (1994) *Biochemistry 33*, 5128−5145.
18. Shibayama, N., Morimoto, H., and Miyazaki, G. (1986) *J. Mol. Biol. 192*, 323−329.
19. Shibayama, N., Imai, K., Morimoto, H., and Satoshi, S. (1995) *Biochemistry 34*, 4773−4780.
20. Olson, J. S., Andersen, M. E., and Gibson, Q. H. (1971) *J. Biol. Chem. 246*, 5919−5923.
21. Gibson, Q. H., and Roughton, F. J. W. (1957) *Proc. R. Soc. London, Ser. B 146*, 206−224.
22. Gibson, Q. H., and Edelstein, S. J. (1987) *J. Biol. Chem. 262*, 516−519.
23. Viggiano, G., Ho, N. T., and Ho, C. (1979) *Biochemistry 18*, 5238−5247.
24. Viggiano, G., and Ho, C. (1979) *Proc. Natl. Acad. Sci. U.S.A. 76*, 3873−3877.
25. Mozzarelli, A., Rivetti, C., Rossi, G. L., Eaton, W. A., and Henry, E. R. (1997) *Protein Sci. 6*, 484−489.
26. Bettati, S., and Mozzarelli, A. (1997) *J. Biol. Chem. 272*, 32050−32055.

BI982970T